Microbiology, March 2016 162: 552-563,
doi: 10.1099/mic.0.000239

Microbiology

Sinorhizobium meliloti low molecular weight phosphotyrosine phosphatase SMc02309 modifies activity of the UDP-glucose pyrophosphorylase ExoN involved in succinoglycan biosynthesis

--Manuscript Draft--

Manuscript Number:	MIC-D-15-00410R1
Full Title:	Sinorhizobium meliloti low molecular weight phosphotyrosine phosphatase SMc02309 modifies activity of the UDP-glucose pyrophosphorylase ExoN involved in succinoglycan biosynthesis
Short Title:	S. meliloti Wzb-like phosphotyrosine phosphatase
Article Type:	Standard
Section/Category:	Physiology and metabolism
Corresponding Author:	Edgardo Jofré Universidad Nacional de Río Cuarto Río Cuarto, Có ARGENTINA
First Author:	Daniela B. Medeot
Order of Authors:	Daniela B. Medeot
	Maria Romina Rivero
	Eugenia Cendoya
	Bruno Contreras-Moreira
	Fernando A. Rossi
	Sonia E. Fischer
	Anke Becker
	Edgardo Jofré
Abstract:	In Gram-negative bacteria, tyrosine phosphorylation has been shown to play a role in the control of exopolysaccharide (EPS) production. This report demonstrates that the chromosomal open reading frame SMc02309 from Sinorhizobium meliloti 2011, encodes a protein with significant sequence similarity to low molecular weight protein tyrosine phosphatases (LMW-PTPs), such as the Escherichia coli Wzb. Unlike other well-characterized EPS biosynthesis gene clusters, which contain neighboring LMW-PTPs and kinase, the S. meliloti succinoglycan (EPS I) gene cluster located on megaplasmid pSymB does not encode a phosphatase. Biochemical assays revealed that the SMc02309 protein hydrolyzes p-nitrophenyl phosphate (p-NPP) with kinetic parameters similar to other bacterial LMW-PTPs. Furthermore, we show evidence that SMc02309 is not the LMW-PTP of the bacterial tyrosine-kinase (BY-kinase) ExoP. Nevertheless ExoN, a UDP-glucose pyrophosphorylase involved in the first stages of EPS I biosynthesis, is phosphorylated at tyrosine residues and constitutes an endogenous substrate of the SMc02309 protein. Additionally, we show that the UDP-glucose pyrophosphorylase activity is modulated by SMc02309-mediated tyrosine dephosphorylation. Moreover, a mutation in the SMc02309 gene decreases EPS I production and delays nodulation on M. sativa roots.

Microbiology, March 2016 162: 552-563,
doi: 10.1099/mic.0.000239

Sinorhizobium meliloti low molecular weight phosphotyrosine phosphatase SMc02309 modifies activity of the UDP-glucose pyrophosphorylase ExoN involved in succinoglycan biosynthesis

Running title: *S. meliloti* Wzb-like phosphotyrosine phosphatase

Daniela B. Medeot[1,2], María Romina Rivero[1], Eugenia Cendoya[1], Bruno Contreras-Moreira[3], Fernando A. Rossi[1], Sonia E. Fischer[1], Anke Becker[4] and Edgardo Jofré[1]*

[1]Department of Natural Sciences, FCEFQyN, National University of Río Cuarto, Ruta Nacional 36 Km 601, Córdoba, Argentina

[2]Department of Molecular Biology, FCEFQyN, National University of Río Cuarto, Ruta Nacional 36 Km 601, Córdoba, Argentina

[3]Laboratory of Computational Biology, Department of Genetics and Plant Production, Estación Experimental de Aula Dei/CSIC, Av. Montañana 1005, Zaragoza

[4]LOEWE-Center for Synthetic Microbiology, Philipps-Universität Marburg, D-35032 Marburg, Germany

***For correspondence: e-mail, ejofre@exa.unrc.edu.ar**

Keywords: Phosphotyrosine-protein phosphatase; Exopolysaccharides; Bacterial protein phosphorylation; Symbiosis

Contents category: Physiology and metabolism

Number of words in the summary: 179

Number of words in the main text: 5931

Number of tables: 3

Number of figures: 5

ABSTRACT

In Gram-negative bacteria, tyrosine phosphorylation has been shown to play a role in the control of exopolysaccharide (EPS) production. This report demonstrates that the chromosomal open reading frame SMc02309 from *Sinorhizobium meliloti* 2011, encodes a protein with significant sequence similarity to low molecular weight protein tyrosine phosphatases (LMW-PTPs), such as the *Escherichia coli* Wzb. Unlike other well-characterized EPS biosynthesis gene clusters, which contain neighboring LMW-PTPs and kinase, the *S. meliloti* succinoglycan (EPS I) gene cluster located on megaplasmid pSymB does not encode a phosphatase. Biochemical assays revealed that the SMc02309 protein hydrolyzes *p*-nitrophenyl phosphate (*p*-NPP) with kinetic parameters similar to other bacterial LMW-PTPs. Furthermore, we show evidence that SMc02309 is not the LMW-PTP of the bacterial tyrosine-kinase (BY-kinase) ExoP. Nevertheless ExoN, a UDP-glucose pyrophosphorylase involved in the first stages of EPS I biosynthesis, is phosphorylated at tyrosine residues and constitutes an endogenous substrate of the SMc02309 protein. Additionally, we show that the UDP-glucose pyrophosphorylase activity is modulated by SMc02309-mediated tyrosine dephosphorylation. Moreover, a mutation in the SMc02309 gene decreases EPS I production and delays nodulation on *M. sativa* roots.

INTRODUCTION

Tyrosine phosphorylation is a reversible and dynamic process, governed by the activities of protein-tyrosine kinases (PTKs), and by two main classes of protein-tyrosine phosphatases: the conventional eukaryotic-like phosphatases and the acidic phosphatases of low molecular weight (LMW-PTPs) (Zhang, 2001).

In bacteria, the genes encoding the LMW-PTP and PTK pairs are generally included in large operons involved in the production or regulation of exopolysaccharides and capsular polysaccharides (CPS). Several studies have reported a direct relationship between the reversible tyrosine phosphorylation and the production of these polymers (Whitfield, 2006; Yother, 2011), which have been identified as significant virulence determinants in many plant and animal pathogens and are also required for symbiotic interactions in plant-associated bacteria (Skorupska *et al.,* 2006). Additionally, many LMW-PTPs and PTKs are also involved in biofilm formation and community development (Whitmore & Lamont, 2012).

In *Escherichia coli*, Wzc and Etk are PTKs essential for the assembly of the group 1 and 4 CPS, respectively (Nadler *et al.,* 2012). In addition to be able to autophosphorylate, PTKs can also phosphorylate endogenous proteins such as sugar-dehydrogenases or -transferases involved in the initial stages of polysaccharide biosynthesis. Indeed, one of the first identified substrates of PTKs was UDP-glucose dehydrogenase (Ugd) of *E. coli* (Grangeasse *et al.,* 2003; Minic *et al.,* 2007).

Wzc and Etk are dephosphorylated by the LMW-PTPs Wzb and Etp, respectively. These proteins have been identified in a number of bacterial species (Kennelly, 2001; Kenelly, 2002; Shi *et al.,* 1998; Ferreira *et al.,* 2007; Preneta *et al.,* 2002; Tan *et al.,* 2013). In addition to Wzc, Wzb dephosphorylates tyrosine residues from Ugd, thus influencing the CPS production (Lacour *et al.,* 2008).

Sinorhizobium meliloti is a Gram-negative soil bacterium belonging to the α-proteobacteria group, which includes other bacteria interacting with eukaryotic hosts, such as *Agrobacterium tumefaciens* or *Brucella* spp. (Moreno *et al.*, 1990). *S. meliloti* is able to establish a symbiosis with alfalfa plants, and fixes molecular nitrogen in root nodules enhancing plant growth and agricultural productivity. In the *S. meliloti-Medicago sativa* symbiosis succinoglycan production is essential during the early stages of bacterial infection and root invasion (Battisti *et al.*, 1992; Gonzalez *et al.*, 1996; Leigh & Walker, 1994; Leigh & Lee, 1988; Niehaus & Becker, 1998).

The biosynthetic pathways of *S. meliloti* EPS I, capsules of *Klebsiella pneumoniae* and group 1-like EPS of *E. coli* (colanic acid) and *Erwinia amylovora* (amylovoran) (Paiment *et al.*, 2002) have similarities. Biosynthesis of EPS I is directed by the *exo* and *exs* genes, which are grouped on megaplasmid pSymB (Becker *et al.*, 1995; Becker *et al.*, 1993). According to the assembly and translocation systems described for polysaccharides, and the genomic localization of the *exoPQT* genes, a Wzy-dependent pathway was proposed for *S. meliloti* EPS I biosynthesis (Reuber & Walker, 1993; Whitfield 2006; Skorupska *et al.*, 2006; Ferreira *et al.*, 2007). In several bacteria—such as *Acinetobacter* sp., *Erwinia amylovora*, *Klebsiella pneumonia*, *Bacillus subtillis* and *Staphylococcus aureus*—a number of PTKs and their respective LMW-PTPs have been characterized (Grangeasse *et al.*, 1998; Bugert & Geider, 1997; Preneta *et al.*, 2002; Mijakovic *et al.*, 2005; Gruszczyk *et al.*, 2011). In *S. meliloti* 2011, the PTKs ExoP and ExoP2 have been described (Niemeyer & Becker, 2001; Jofré & Becker, 2009). Moreover, the *S. meliloti* genome contains two open reading frames (ORFs), probably encoding LMW-PTPs (Niemeyer & Becker, 2001). The functional properties of these two ORFs, however, have not yet been reported. In the present work, we examined whether one of these *S. meliloti* ORFs—namely SM2011_c02309, hereafter referred to as SMc02309—is a LMW-PTP. We also determined the kinetic parameters as well as the PTP activity on the tyrosine kinase ExoP and on ExoN, a protein involved in the initial stages of succinoglycan

biosynthesis. Finally, we demonstrated the influence of a mutation in the SMc02309 gene on EPS production and symbiotic performance of *S. meliloti* with *M. sativa* plants.

METHODS

Bacterial strains and growth conditions. Table 1 lists the *S. meliloti* strains, primers and plasmids used in this work. The *E. coli* strains were grown at 37°C in Luria-Bertani (Sambrook, 1989).

S. meliloti 2011 and its derivatives were grown at 30°C in TY or glutamate-D-mannitol-salts (GMS) medium (Beringer, 1974; Zevenhuisen & van Neerven, 1983). When required, antibiotics were added at the following concentrations (μg/mL): 10 nalidixic acid (Nx), 10 tetracycline (Tc), 40 gentamicin (Gm), 120 neomycin (Nm) for *S. meliloti*, and 100 ampicillin (Ap), 10 tetracycline, and 50 kanamycin (Km) for *E. coli*.

Plasmids. Standard molecular cloning techniques were used throughout this study (Sambrook, 1989). PCR was performed using standard conditions (Ausubel, 1995) with Pfx platinum Polymerase (Invitrogen). All plasmid constructions generated in this study were verified by sequencing.

The SMc02309 gene—lacking the TGA codon—was amplified by PCR with the primers 2309f, 2309r and the *S. meliloti* strain Rm2011 DNA as template. The resultant 477-bp fragment was digested with *Nde*I-*Sap*I, followed by ligation into *Nde*I-*Sap*I digested pTYB1 (New England Biolabs). In the pTYB-02309, the C-terminus of the target SMc02309 protein was fused to the self-cleavage intein tag containing a chitin binding domain.

In a similar manner, the 906-bp amplicon corresponding to the *exoN* from *S. meliloti* strain Rm2011 (generated by PCR with the primers exoNf and exoNr) was digested with *Nde*I and

*Bam*HI, followed by ligation into *Nde*I-*Bam*HI digested pET28a(+) (Novagen). In the pET-exoN, the N-terminus of the target protein was fused to the 6xHis tag.

Construction of SMc02309 mutant strain. The nonpolar mutant Rm42 was generated by the integration of plasmid pk18-02309 into the SMc02309 coding region of wild-type strain Rm 2011 following *E. coli* S17-1 mediated conjugal plasmid transfer and homologous recombination. The transconjugants were selected for resistance to Nx and Nm. Plasmid pk18-02309 carries an internal 187-bp fragment of SMc02309 gene that was generated by PCR amplification (with the primers pK2309f and pK2309r) and subsequent insertion into the *Eco*RI and *Hind*III restriction sites of plasmid pK18mob2.

Plasmid pFAJ-02309 was constructed by ligation of the *Xba*I-*Kpn*I digested product resulting from PCR amplification of SMc02309 gene (with primers pFAJ2309f, pFAJ2309r and *S. meliloti* strain Rm2011 DNA as template) to the *Xba*I-*Kpn*I digested plasmid pFA1708. Plasmid pFAJ-02309 was mobilized by mating from *E. coli* S17-1 to *S. meliloti* mutant strain Rm42.

Production and purification of the SMc02309-intein fusion protein. For large scale purification, 500 mL of LB supplemented with Ap were inoculated with an overnight culture (1% vol/vol) of *E. coli* BL21 (DE3) containing plasmid pTYB-02309 and then incubated at 37°C with shaking to an OD_{600} of 0.6. The induction was initiated by adding 0.5 mM IPTG (final concentration) with the incubation being continued overnight with shaking at 22°C. The cells were harvested and lysed by sonication in 5 mL column buffer (20 mM HEPES-Na, pH 8.0, 500 mM NaCl, 1 mM Na-EDTA) containing 1 mg mL^{-1} RNaseA and 1 mM PMSF. The resulting cell suspension was centrifuged (100,000 x *g* for 1 h) and the supernatant loaded onto a chitin column (New England Biolabs). After several washings with column buffer, the proteins were eluted with the same buffer previous incubation overnight with 50 mM DTT to induce the autocleavage reaction. The resulting fractions were analyzed by SDS-PAGE, and

154 the purified protein SMc02309 dialyzed against dialysis buffer (10 mM Tris-HCl, pH 8.0 and
155 30% vol/vol glycerol) before concentration by centrifuging in microfiltration tubes (Amicon
156 Ultra, Millipore; molecular-weight cutoff 3,000 Da). Finally, the purified SMc02309 protein
157 was analyzed by SDS-PAGE and stored at -20°C until use.
158
159 **Production and purification of the ExoPc-GST fusion protein.** Production and purification
160 of the ExoPc-GST fusion protein was performed according to described by Niemeyer &
161 Becker (2001). The purified protein was then analyzed by SDS-PAGE before storage at -20°C
162 until use.
163
164 **Production and purification of 6xHis-ExoN.** Briefly, an overnight culture of *E. coli* BL21
165 (DE3) cells containing plasmid pET28-exoN was used to inoculate 100 mL of LB broth
166 supplemented with Km. The cells were next induced with IPTG as described above, then
167 harvested and lysed by sonication in 3 mL of wash buffer (50 mM NaH_2PO_4, 300 mM NaCl,
168 20 mM imidazole, pH 8) containing 1 mg mL^{-1} RNaseA and 1 mM PMSF. The resulting
169 suspension was centrifuged (100,000 x *g* for 1 h) and the supernatant loaded onto an Ni-NTA
170 agarose column (Qiagen). After several washings of the column, the proteins were eluted with
171 the elution buffer (50 mM NaH_2PO_4, 300 mM NaCl, 250 mM imidazole). The fractions were
172 analyzed by SDS-PAGE and the purified ExoN protein was dialyzed and concentrated by
173 centrifugation. Finally, the purified ExoN protein was analyzed by SDS-PAGE before storage
174 at -20°C until use.
175
176 **MALDI-TOF-TOF spectrometry.** The overproduced proteins were separated by SDS-
177 PAGE and the corresponding bands containing the purified proteins submitted to the Center
178 for Chemical and Biological Studies Maldi Tof Spectrometry (CEQUIBIEM-Argentina) for
179 spectrometric analysis in a MALDI-TOF-TOF spectrometer, Ultraflex II (Bruker).

Assays for phosphatase activity. The standard *in vitro* assay to measure acid-phosphatase activity (Preneta *et al*., 2002) was performed at 37°C in a reaction mixture containing, in a total volume of 0.1 mL, 20 mM sodium citrate buffer pH 6.0, 0.1 mM $ZnSO_4$, and 10 mM *p*-NPP. The reactions were incubated for 60 min and then stopped by the addition of sodium hydroxide to 1 M.

The effect of ions on the kinetic reactions was conducted either with or without 0.1 mM of each of the following cations: Ca^{2+}, Cu^{2+}, Fe^{3+}, Fe^{2+}, Mn^{2+}, Mg^{2+}, Ni^{2+} and Zn^{2+}. Also, the PTP inhibitors sodium vanadate and sodium pyrophosphate ($NaPP_i$) were added to the reaction at a final concentrations of 1 and 2.5 mM, respectively.

To determine the optimal pH for phosphatase activity, the sodium acetate (pH 4.2) or the sodium citrate buffer (with pH varying from 5.5 to 7.5) was used. In parallel, the optimal temperature was determined in the range from 30 to 85°C.

Saturation curves with the addition of Zn^{2+} were performed in the presence of a variable concentration of *p*-NPP ranging from 0 to 60 mM. The times of the reactions, amounts of enzyme, and concentrations of substrates were optimized to have linear kinetics. The kinetic parameters Km and Vmax were estimated by non-linear fitting the Michaelis-Menten curve with Origin software. The *p*-nitrophenol levels during a reaction were monitored by the increase in absorbance at 405 nm in a Tecan Infinite M200 reader (Tecan Trading AG). For calculations the molar-extinction coefficient 18,000 M^{-1} cm^{-1} was used (Cirri *et al.,* 1993). One unit of acid phosphatase was defined as the amount of enzyme that released 1 μmol of *p*-nitrophenol from *p*-NPP per min at 37 °C. The protein concentration was determined according to Bradford (1976) with BSA as standard.

Dephosphorylation assays. Dephosphorylation of GST-ExoPc and 6xHis-ExoN was detected by immunoblot analysis. For that, 5 µg of GST-ExoPc or 6xHis-ExoN were incubated at 37 °C for 2h with 5 µg of SMc02309 protein in 25 µL of a buffer containing 20 mM sodium citrate (pH 6) and 0.1 mM zinc sulfate. As a positive control for dephosphorylation, GST-ExoPc and 6xHis-ExoN were incubated with 1 U of the commercial alkaline phosphatase (Fermentas). The reaction was stopped by the addition of an equal volume of 2X SDS-PAGE sample buffer. The mixture was heated at 100 °C for 5 min and subsequently analyzed by SDS-PAGE with immunodetection by means of the monoclonal antiphosphotyrosine-biotinylated antibody (clone PT-66, Sigma).

Immunoblotting analysis. Purified GST-ExoPc and 6xHis-ExoN proteins were separated and analyzed by SDS-PAGE with either subsequent visualization by Coomassie blue R-250 staining or transfer onto PVDF membranes for immunoblotting in a semidry electrophoretic transfer cell, as described by Towbin *et al.* (1979). The GST-ExoPc protein was detected with an ExoP-specific peptide antibody [rabbit] (Eurogentec) raised with the peptide EWGRTPSRLVR. The anti-ExoP antibody was diluted in Tris-buffered saline supplemented with 0.1% (vol/vol) Tween 20 and 0.3% (wt/vol) nonfat dry milk. The binding of the secondary antibody, a biotinylated anti-rabbit immunoglobulin G (GE Healthcare), was detected with streptavidin-biotinylated horseradish peroxidase complex (GE Healthcare). Immunoblots for the 6xHis-ExoN protein were probed with the monoclonal anti-His antibody from mouse (GE Healthcare). The binding of the secondary antibody, the anti-mouse immunoglobulin G peroxidase conjugate (Sigma), was detected by ECL chemiluminescence reagents (Thermo Scientific). Phosphorylation on tyrosine residues was detected with the monoclonal anti-phosphotyrosine-biotinylated antibody (clone PT-66 Sigma).

Assays for UDP-Glucose pyrophosphorylase activity. 6xHis-ExoN protein was tested for UDP-glucose pyrophosphorylase activity by using a spectrophotometric assay as described elsewhere (Bergmeyer et al., 1983). Briefly, the 100 µL reaction mixture contained 100 mM MOPS buffer (pH 7.6), 1.5 mM $MgCl_2$, 0.38 mM NADP, 20 µM glucose 1,6-diphosphate, 0.9 U of glucose 6-phosphate dehydrogenase, 6.6 U of phosphoglucomutase, 1 µmol of UDP-glucose, and 0.9 µg of 6xHis-ExoN. The reaction was started by adding 1.5 µmol of PP_i. The absorbance at 340 nm was measured for 15 min by using an Epoch Microplate Spectrophotometer (BioTek). The endogenous NADPH-oxidation rates were subtracted from the 6xHis-ExoN -induced NADPH values.

UDP-glucose pyrophosphorylase activity was also determined after dephosphorylating of 6xHis-ExoN. For this purpose, 0.9 µg of 6xHis-ExoN was either dephosphorylated with 2 µg of SMc02309 or with 1 U of the commercial alkaline phosphatase (ALP) by incubating 6xHis-ExoN for 10 min in reaction mixture prior the determination of UDP-glucose pyrophosphorylase activity.

Analysis of the EPS I content and distribution. EPS I was obtained from dialyzed supernatants (molecular-weight cutoff of 2,000) from 6-day-old cultures grown in GMS medium supplemented with 240 mM NaCl (Jofré & Becker, 2009). Total carbohydrates were determined by the anthrone method (Dische, 1962).

Nodulation assays. *S. meliloti* strains were assayed for their symbiotic phenotypes on *M. sativa* cv. Monarca (obtained from the Instituto Nacional de Tecnología Agropecuaria, Argentina). The seeds were surface sterilized and germinated as described by Müller *et al.*, (1988). Inoculation of seedlings was carried out with log-phase cultures. The plantlets were grown on nitrogen free medium as described by Rolfe *et al.*, (1980). Nodule formation was assayed over four weeks.

Bioinformatics tools. DNA and protein data were analyzed through the use of the ORF-finder tool located at the National Center for Biotechnology Information (NCBI). The algorithm BLAST was used to compare the deduced amino-acids sequences to those available in the NCBI database. Structure predictions and general protein characteristics were obtained from the Expasy server (http://www.expasy.org). Conserved ortholog neighborhood regions were obtained from the Integrated Microbial Genomes (IMG) system (Markowitz *et al.*, 2006) available at http://img.jgi.doe.gov.

Pairwise alignments between the SMc02309 protein and Protein Data Bank template structures (1jl3_A, 1zgg_A , 2cwd_A, 2fek_A, 2ipa_B, 2wja_A, 2wmy_A, 3rh0_A , 3rof_A and 3t38_A) were calculated with HHpred (Söding *et al.*, 2005) and subsequently formatted as input for the software Modeller 9v10 (Sali *et al.*, 1995). The resulting top model was predicted by ModEval (Eramian *et al.*, 2008) to have a root-mean-square-deviation (RMSD) value of 4.552. In order to check the potential binding sites of this model the ligands present in PDB entry 2WJA were merged to give the resulting final model.

Statistical analyses. All experiments were performed at least in triplicate. Data are presented as means ± SD of the indicated number of experiments. Statistical analyses were done by Student's t-test and one-way analysis of variance and the means were compared by the Tukey´s test.

RESULTS

In *Sinorhizobium meliloti* the genes encoding the ExoP tyrosine-kinase and the putative phosphotyrosine phosphatase SMc02309 are not genetically linked

In *S. meliloti*, the PTP that dephosphorylates the C-terminal domain of the PTK ExoP has not yet been identified (Grangreasse *et al.*, 2007). A gene neighborhood analysis clearly indicated the absence of PTP homologs located upstream from *exoP* (Fig. S1a). Therefore, *S. meliloti* does not possess the same genetic arrangement with regard to the BY-kinase and PTP loci that has been observed in other bacterial species (Huang & Schell, 1995; Grangeasse *et al.*, 1998; Vincent *et al.*, 1999; Ferreira *et al.*, 2007; Arakawa *et al.*, 1995; and Bugert & Geider, 1995). This result prompted us to initiate a genome search to identify putative candidates encoding PTPs in *S. meliloti*. We detected a *S. meliloti* chromosomal ORF (locus tag SM2011_c02309, in this work referred to as SMc02309) containing pfam01451, a highly conserved domain in the well characterized tyrosine-phosphatase Wzb from *E. coli*. The predicted SMc02309 protein was originally annotated as a putative arsenate reductase—as inferred by automated annotation—although SMc02309 is not included within the *ars* operon. BLASTP sequence analysis revealed that SMc02309 is significantly similar to other biochemically characterized LMW-PTPs and a synteny analysis of the SMc02309 gene showed conserved neighbouring orthologous genes when compared with other rhizobia and *Brucella* strains (Fig. S1b). The SMc02309 protein shares: 1) the conserved motif $CX_5R(S/T)$ in the active site, including the arginine residue crucial for the binding of the phosphate substrate (Kennelly & Potts, 1999) and a conserved cysteine residue required for the enzymatic activity (Zhang *et al.*, 1994), and 2) an invariant aspartate in DP(Y/T) motif (positions 116 in Wzb and 120 in Smc02309) (Fig. S1c). Furthermore, the SMc02309 protein is included in the tyrosine-phosphatase group and appears to be close to the LMW protein phosphatase encoded by the locus tag Q57FA1/BruAb1_0278 of *Brucella abortus* (Fig. S2).

Taken together, these predictions suggest that the SMc02309 protein might be an LMW-PTP in *S. meliloti*.

The molecular structure of SMc02309 resembles the LMW-PTP Wzb from *E. coli*

Analysis by Homology Detection and Structure Prediction (HHPred; Söding *et al.*, 2005) of the amino-acid sequence of the SMc02309 predicted three β-sheets and three α-helices. Scans within the Protein Data Bank revealed that this protein is significantly similar to other arsenate reductase enzymes and amino-acid phosphatases, but with rather low sequence identity (20-30%). Nevertheless, whereas SMc02309 does not conserve all the essential catalytic cysteine residues present among the former enzymes, the protein does contain a CX5R(S/T) motif, which forms the phosphate binding loop in the active site (known as the P-loop) present among the LMW-PTPs (*cf.* above). Therefore, on the basis of sequence conservation, it seems more likely that this protein might be an LMW-PTP. Among the phosphatases with experimentally determined three-dimensional structures found in our searches, the most similar protein was Wzb (2WJA PDB entry). The superimposition of Wzb upon the model of SMc02309 was consistent with the hypothesis of SMc02309 being a phosphatase (data not shown).

SMc02309 from *S. meliloti* is an acid phosphatase: optimal conditions for *in vitro* activity

In vitro enzymatic assays with purified SMc02309 protein were performed to test for the predicted LMW-PTP activity. The SMc02309 gene from *S. meliloti* 2011 lacking the stop codon was amplified and cloned into the expression vector pTYB1. SDS-PAGE analysis of proteins from *E. coli* cultures induced with IPTG exhibited an overproduction of a 70-kDa protein consistent with the expected mass for the SMc02309 intein-tagged fusion protein. After affinity purification and on-column cleavage with DTT, a 17-kDa protein corresponding to the predicted mass for SMc02309, was eluted (Fig. 1a). Mass spectrometry analysis after tryptic digestion of the SMc02309 yielded peptides in which the m/*z* data observed were in good agreement with the theoretical values expected for SMc02309 (Fig. 1b). The results

revealed that the purified protein corresponded to SMc02309 at a P-value of $1E^{-107}$ (0.05 significance cut off< $1E^{-82}$).

In vitro characterization of the SMc02309 protein included the following determination of the most favorable conditions for phosphatase activity. The purified SMc02309 protein was active in *p*-nitrophenyl phosphate (*p*-NPP) hydrolysis, with the resulting activity for 1 h at 37°C being the most stable at 40 μg/mL of enzyme. The Km and Vmax were determined through non-linear fit function on V vs. [S] curve. The Vmax for the specific activity of SMc02309, measured at pH 6 in presence of 0.1 mM Zn^{+2}, was 135.17 U (mg protein)$^{-1}$. A Km of 10.88 mM was estimated by means of a saturation curve of *p*-NPP hydrolysis in the presence of the cofactor Zn^{+2} (Fig. 2a). The Km obtained indicated that the SMc02309 phosphatase had a higher affinity in the presence of Zn^{2+} and Fe^{3+} than with Cu^{2+}. Moreover, Mn^{2+}, when added, had no significant effect (data not shown). The optimal *p*-NPP hydrolysis occurred at pH 6 (Fig. 2b) and 37°C (Fig. 2c). A very low residual activity was observed, however, at 65°C. Regarding PTP inhibitors, 1 mM Na_3VO_4 and 2.5 mM $NaPP_i$ were efficient inhibitors of the SMc02309 phosphatase activity (Table 2).

We also tested arsenate reductase activity by measuring NADPH oxidation (Anderson & Cook, 2004) and after three independent experiments concluded that SMc02309 does not catalyze that reaction (data not shown).

SMc02309 is not the phosphotyrosine phosphatase of the tyrosine kinase ExoP

In order to assess whether SMc02309 exhibited phosphotyrosine phosphatase activity on ExoP, we proceeded to overexpress the *exoP* sequence encoding for the C-terminal domain of ExoP as a GST-fusion protein (GST-ExoPc). For dephosphorylation assays, GST-ExoPc was incubated in presence or absence of SMc02309 for 2 h. We were then able to show by immunoblotting that the GST-ExoPc fusion protein was indeed phosphorylated on tyrosine

residues, as revealed by a monoclonal antiphosphotyrosine antibody (Fig. 3a). Furthermore, we found that SMc02309 did not dephosphorylate GST-ExoPc. In contrast, commercial alkaline phosphatase (ALP) produced a complete dephosphorylation of the GST-ExoPc fusion protein under the same conditions. The GST-ExoPc was detected by immunoblotting with the anti-ExoP polyclonal antibody.

The SMc02309 acid phosphatase dephosphorylates tyrosine residues of the ExoN protein

ExoN is a UDP glucose pyrophosphorylase that catalyzes the conversion of glucose 1-phosphate into UDP-glucose—the latter being a precursor in EPS I biosynthesis (Becker *et al.,* 1993). In addition, the ExoN amino-acid sequence contains seven tyrosine residues that are potential targets for phosphorylation. Therefore, we determined whether ExoN was phosphorylated on tyrosine residues, as well as whether ExoN could be an endogenous substrate for SMc02309. To demonstrate the predicted activity of SMc02309 as a phosphotyrosine phosphatase of ExoN, the *exoN* gene was overexpressed to produce a 6xHis-ExoN recombinant protein that was subsequently purified. The 33 kDa protein obtained was identified—by MALDI-TOF-TOF mass spectrometry—as being consistent with ExoN from *S. meliloti*. Although 6xHis-ExoN usually resulted in a double band on SDS-PAGE analysis, both bands were identified as ExoN.

We performed immunoblotting of 6xHis-ExoN either with or without a previous incubation with the SMc02309 protein (Fig. 3b) and did likewise with ExoPc. The ExoN protein was phosphorylated at tyrosine residues as detected by using the monoclonal antiphosphotyrosine antibody (Fig. 3b). Furthermore, the degree of ExoN tyrosine phosphorylation decreased when the protein was incubated in presence of the acid phosphatase SMc02309, whereas a complete dephosphorylation of ExoN was observed in presence of ALP. Since both ExoN bands were detected as tyrosine-phosphorylated and they were dephosphorylated by both

382 phosphatases, we speculate that the slight difference in mass could be the result of differences
383 in the degree of tyrosine phosphorylation.
384 In all these incubations, the 6xHis-ExoN was detected by immunoblotting with the anti-His
385 monoclonal antibody (GE Healthcare).
386 *In vitro* UDP glucose pyrophosphorylase activity of ExoN was considerably reduced when the
387 protein was previously incubated with either SMc02309 or ALP phosphatases (Table 3).
388 Taken together, these results evidenced that: 1) the ExoN protein was phosphorylated on
389 tyrosine residues, 2) SMc02309 indeed exhibited tyrosine-phosphatase activity on ExoN and
390 3) ExoN dephosphorylation by SMc02309 could be physiologically relevant because it
391 negatively affected the enzymatic activity of ExoN *in vitro*.
392
393 **A nonpolar mutant for SMc02309 gene affects EPS I production**
394 To determine the potential role of SMc02309 gene in EPS I production and symbiosis with *M.*
395 *sativa*, we generated the mutant strain Rm42 by site-directed plasmid integration in which the
396 *lac* promoter of plasmid pK18mob2 was driving transcription of the gene downstream of
397 SMc02309. At 28 °C, no differences in growth rate were observed in the Rm42 mutant in
398 comparison to the parental strain Rm2011 (data not shown). EPS I production was measured
399 in 6-days-old culture supernatants from GMS medium supplemented with 240 mM NaCl (an
400 optimal condition for EPS I production). Rm42 accumulated significantly less EPS I
401 compared to the Rm2011 wild-type. As expected, complementation of the Rm42 mutant
402 strain with the wild type allele (Rm43) restored EPS production.
403 Extended incubation (9-days-old) was also attempted but the results were ambiguous,
404 possibly due to changes in the medium that can affect EPS I production at the transcriptional
405 level (Geddes *et al.*, 2014). To exclude the possibility that plasmid pFAJ1708 influences the
406 EPS I production, we included *S. meliloti* strain Rm148 harbouring empty pFAJ1708 as a
407 control. In addition, to confirm that the hexose equivalents measured were derived from EPS

I, the *S. meliloti exoY* mutant (strain RmAR9007), deficient in production of EPS I (Keller *et al.*, 1995), was included as another control (Fig. 4).

Nodulation of *Medicago sativa* roots is delayed in nonpolar mutant for SMc02309 gene

EPS I in *S. meliloti* plays an essential role in nodule invasion. Mutants affected in EPS I biosynthesis give symbiotic phenotypes that range from non-invasive (e.g., *exoY* mutation) to not detectable (e.g., *exoX* mutation), the latter being capable of inducing the formation of nitrogen-fixing nodules on the host plant alfalfa (Reed *et al.*, 1991). More recently it has been shown that increased EPS synthesis can be beneficial for symbiosis (Jones *et al.*, 2012). Since *exoN* mutants have been shown to be symbiotically proficient, and SMc02309 appears to affect the amount of EPS I being synthesized, we hypothesized that a mutation might lead to a delay in nodulation. To test this hypothesis, the symbiotic proficiency of mutant Rm42 was compared with that of wild-type Rm2011. Although both strains established an effective symbiosis, as evidenced by the presence of pink and elongated nodules, the mutant strain Rm42 exhibited a significant delay in nodulation of *M. sativa* roots (Fig. 5).

DISCUSSION

In proteobacteria, genes encoding LMW-PTPs are often located immediately upstream from the genes encoding the BY-kinases (Grangeasse *et al.*, 1998; Whitfield 2006). In *S. meliloti*, the chromosomal gene SMc02309 encoding a potential phosphatase is genetically not linked to *exoP* located on megaplasmid pSymB, suggesting that SMc02309 may not be specific for ExoP. The deduced amino-acid sequence of SMc02309 shares 30% identity and 43% similarity with the *E. coli wzb*-encoded enzyme (Niemeyer & Becker, 2001).

Furthermore, biochemical analyses demonstrated that SMc02309 is able to hydrolyze the artificial substrate *p*-NPP, a commonly used substrate in phosphatase *in vitro* assays (Bennett *et al.*, 2001; Mori *et al.*, 2012; Standish & Morona, 2014). The estimated Km and Vmax values obtained for SMc02309 were similar to those described for the LMW-PTP BceD of *Burkholderia cepacia* (Ferreira *et al.*, 2007), the Wzb of *Acinetobacter iwoffii* (Nakar & Gutnick 2003), the Yor5 *of Klebsiella pneumonia* (Preneta *et al.*, 2002), the Wzb of *E. coli* (Vincent *et al.*, 1999) and the Ptp of *Acinetobacter johnsonii* (Grangeasse *et al.*, 1998). In addition, the optimal pH and temperature values for catalytic activity resemble those for the above-mentioned bacterial Cys-based protein phosphatases. The presence of Fe^{3+} or Cu^{2+} ions also significantly increased SMc02309 activity; while the presence of Zn^{2+} ions, a phosphatase cofactor, increased the activity by almost three-fold. Na_3VO_4 was an efficient inhibitor of SMc02309. The described pattern of sensitivity to inhibitors is in line with the reported properties of other PTPs, such as the *Bacillus subtilis* protein tyrosine phosphatase YwqE (Mijakovic *et al*., 2005).

Protein phosphorylation plays a role during pathogenic or symbiotic processes, (Grangeasse *et al.*, 2007). A major breakthrough has been made by demonstrating a biologic link between the activities of certain protein-tyrosine kinases and phosphatases and the production and/or transport of surface polysaccharides (Cozzone 2005; Standish & Morona, 2014). Therefore, we explored a putative functional link between the activity of SMc02309 and the protein-tyrosine kinase ExoP from *S. meliloti.* It was reported that the molecular-weight distribution of EPS I is altered by amino acid substitutions in the tyrosine residues of the C-terminal domain of ExoP (Niemeyer & Becker 2001). Nevertheless, the SMc02309 phosphatase was not able to dephosphorylate the C-terminal domain of ExoP, suggesting that the SMc02309 phosphatase is not the cognate LMW-PTP of the BY-kinase ExoP. This observation is further supported by the fact that SMc02309 and *exoP* genes are not genetically linked.

In order to assess the implication of SMc02309 on polysaccharides biosynthesis we looked for possible substrates in this process. In several bacteria, UDP-glucose dehydrogenases (Ugd) catalyze the formation of glucuronic acid, whose product serves as a building block for polysaccharides biosynthesis. The transphosphorylation of Ugd of *E. coli* by the tyrosine kinase Wzc is highly relevant because the phosphorylated state of Ugd (Ugd-P) increases its enzymatic activity; thus enhancing synthesis of UDP-glucuronic acid, a substrate in the production of colanic acid. Ugd-P also serves as a substrate for the LMW-PTP Wzb (Grangeasse *et al.,* 2003, Lacour *et al.,* 2008). In *S. meliloti*, ExoN functions as a UDP-glycosyl pyrophosphorylase involved in the synthesis of UDP-glucose from glucose 1-phosphate (Glucksmann *et al.,* 1993). Here, we demonstrate that ExoN is phosphorylated on tyrosine residues and SMc02309 phosphatase dephosphorylates ExoN. *In vitro* assays also demonstrated that the enzymatic activity of ExoN is negatively modulated by tyrosine dephosphorylation. In concordance with our results, the UDP-glucose dehydrogenase activity of *E. coli* Ugd was severely reduced by dephosphorylation mediated by Wzb (Grangeasse *et al.,* 2003).

Our results suggest that in *S. meliloti* the enzymatic activity of ExoN—required for activation of the precursors of EPS I—is modulated by phosphorylation-dephosphorylation cycles, with the latter step being mediated by the SMc02309 phosphotyrosine phosphatase.

Standish & Morona (2014) reviewed that both deletion and overexpression of phosphatases alter exopolysaccharide biosynthesis in a broad range of bacteria. For example, in addition to changes in Wzb levels affecting EPS biosynthesis in *E. coli* (Vincent *et al.*, 1999; Vincent *et al.*, 2000), in *Streptococcus thermophilus* a lack of the EpsB phosphatase results in a slight reduction in the amount of EPS was reported (Minic *et al.,* 2007). In contrast, PhpA, a tyrosine phosphatase of *Myxococcus xanthus*, was recently reported to be a putative negative regulator of EPS production (Mori *et al.,* 2012).

The lower levels of EPS I synthesis, observed in the mutant strain affected in SMc02309, may affect early nodulation since a decrease in UDP-glucose subunits should lead to decreased production of EPS I as well as a delay in nodulation. Jones (2012) demonstrated that enhanced production of EPS I improves symbiosis of *S. meliloti* with *M. truncatula*. More recently, Geddes *et al*. (2014) suggested that an increased accumulation of EPS I can have a positive effect on nodulation and competition for nodule occupancy.

Since the *S. meliloti* genome contains another gene, ExoN2, encoding a probable UDP-glycosyl pyrophosphorylase; the possibility that ExoN2 is also a substrate for SMc02309 cannot be excluded and should be investigated. Moreover, the weak change of EPS production in the SMc02309 mutant could be the result of compensation effects caused by the enzymatic activity of ExoN2.

Recently, strong evidence for a critical role of PTPs in Wzy-dependent capsule production was reported in several bacteria. Moreover, the discovery of small molecules inhibitory to the activity of PTPs—in both Gram-positive and Gram-negative pathogens—suggest that these PTPs constitute suitable targets for the development of antivirulence drugs (Standish *et al.,* 2012). The evidence implying that SMc02309 acts as a phosphatase mediating cell signalling events in *S. meliloti*, though preliminary, is promising. In summary, this report described for the first time phosphatase characteristics of SMc02309, a protein annotated as a putative arsenate reductase of *S. meliloti* and suggests that ExoN is one of the endogenous substrates. Further studies will be required to unravel whether or not SMc02309 affects signalling pathways regulating interactions with the eukaryotic host and EPS biosynthesis.

ACKNOWLEDGMENTS

This work was funded by grants from the Consejo Nacional de Investigaciones Científicas y Técnicas (CONICET), Argentina and the Secretaría de Ciencia y Técnica de la Universidad

Nacional de Río Cuarto, Argentina. D.B.M., M.R.R., E.J. and S.E.F. are members of the Research Career from CONICET. E.C. and F.A.R. are scholarships recipient's from CONICET. A.B. was supported by the German Research Foundation (Collaborative Research Centre 987) and the LOEWE program of the State of Hesse (Germany). The authors wish to thank Dr. Donald F. Haggerty for editing the manuscript.

REFERENCES

Altschul, S. F., Gish, W., Miller, W., Myers, E. W. & Lipman, D. J. (1990). Basic local alignment search tool. *J Mol Biol* **215**, 403-410.

Anderson, C. R. & Cook, G. M. (2004). Isolation and characterization of arsenate-reducing bacteria from arsenic-contaminated sites in New Zealand. *Curr Microbiol* **48,** 341-347.

Arakawa, Y., Wacharotayankun, R., Nagatsuka, T., Ito, H., Kato, N. & Ohta, M. (1995). Genomic organization of the *Klebsiella pneumonia cps* region responsible for serotype K2 capsular polysaccharide synthesis in the virulent strain Chedid. *J Bacteriol* **177**, 1788-1796.

Ausubel, F. M., Brent, R., Kingston, R. E., *et al.*, (Eds). (1995). Current Protocols in Molecular Biology, John Wiley & Sons, New York.

Battisti, L., Lara, J. C. & Leigh, J. A. (1992). Specific oligosaccharide form of the *Rhizobium meliloti* exopolysaccharide promotes nodule invasion in alfalfa. *Proc Natl Acad Sci U S A* **89**, 5625-5629.

Becker, A., Kleickmann, A., Keller, M., Arnold, W. & Pühler, A. (1993). Identification and analysis of the *Rhizobium meliloti exoAMONP* genes involved in exopolysaccharide

biosynthesis and mapping of promoters located on the *exoHKLAMONP* fragment. *Mol Gen Genet* **241**, 367-379.

Becker, A., Niehaus, K. & Pühler, A. (1995). Low molecular weight succinoglycan is predominantly produced by *Rhizobium meliloti* strains carrying a mutated ExoP protein characterized by a periplasmic N-terminal and a missing C-terminal domain. *Mol Microbiol* **16**, 191-203.

Bennett, M. S., Guan, Z., Laurberg, M. & Su, X. D. (2001). *Bacillus subtilis* arsenate reductase is structurally and functionally similar to low molecular weight protein tyrosine phosphatases. *Proc Natl Acad Sci U S A* **98,** 13577-13582.

Bergmeyer, H. U., Graβl, M. & Walter H.-E. (1983). Uridinediphosphoglucose pyrophosphorylase, p. 324-326. **In H. U. Bergmeyer (ed.),** Methods in enzymatic analysis, 3rd ed., vol. 2. Verlag Chemie, Weinheim, Germany.

Beringer, J. E. (1974). R factor transfer in *Rhizobium leguminosarum*. *J Gen Microbiol* **84,** 188-198.

Bradford, M. (1976). A rapid and sensitive method for quantitation of microgram quantities of protein utilizing the principle of protein-dye binding. *Anal Biochem* **72,** 248-254.

Bugert, P. & Geider, K. (1995). Molecular analysis of the *ams* operon required for exopolysaccharide synthesis of *Erwinia amylovora*. *Mol Microbiol* **15,** 917-933.

559 **Bugert, P. & Geider, K. (1997).** Characterization of the *amsI* gene product as a low
560 molecular weight acid phosphatase controlling exopolysaccharide synthesis of *Erwinia*
561 *amylovora*. *FEBS Lett* **400,** 252-256.
562
563 **Chao, J. D., Wong D. & Av-Gay, Y. (2014).** Microbial Protein-tyrosine Kinases
564 *J Biol Chem* **289,** 9463-9472.
565
566 **Cirri, P., Chiarugi, P., Camici, G., Manao, G., Raugei, G., Cappugi, G. & Ramponi, G.**
567 **(1993).** The role of Cys12, Cys17 and Arg18 in the catalytic mechanism of low-M(r)
568 cytosolic phosphotyrosine protein phosphatase. *Eur J Biochem* **214,** 647-657.
569
570 **Cozzone, A. J. (2005).** Role of protein phosphorylation on serine/threonine and tyrosine in
571 the virulence of bacterial pathogens. *J Mol Microbiol Biotechnol* **9,** 198-213.
572
573 **Daniels, R., Reynaert, S., Hoekstra, H., Verreth, C., Janssens, J., Braeken, K., Fauvart,**
574 **M., Beullens, S., Heusdens, C., Lambrichts, I., De Vos, D. E., Vanderleyden, J.,**
575 **Vermant, J. & Michiels, J. (2006).** Quorum signal molecules as biosurfactants affecting
576 swarming in *Rhizobium etli*. *Proc Natl Acad Sci U S A* **103,** 14965-14970.
577
578 **Dische, Z. (1962).** General color reactions. *Methods Carbohyd Chem* **1,** 478-492.
579
580 **Eramian, D., Eswar, N., Shen, M. Y. & Sali, A. (2008).** How well can the accuracy of
581 comparative protein structure models be predicted? *Protein Sci* **17,** 1881-1893.
582
583 **Ferreira, A. S., Leitão, J. H., Sousa, S. A., Cosme, A. M., Sá-Correia, I. & Moreira, L.**
584 **M. (2007).** Functional analysis of *Burkholderia cepacia* genes *bceD* and *bceF*, encoding a

phosphotyrosine phosphatase and a tyrosine autokinase, respectively: role in exopolysaccharide biosynthesis and biofilm formation. *Appl Env Microbiol* **73,** 524-534.

Geddes, B. A., González, J. E. & Oresnik, I. J. (2014). Exopolysaccharide production in response to medium acidification is correlated with an increase in competition for nodule occupancy. *Mol Plant-Microbe Interact* **27,** 1307-1317.

Glucksmann, M. A., Reuber, T. L. & Walker, G. C. (1993). Genes needed for the modification, polymerization, export, and processing of succinoglycan by *Rhizobium meliloti*: a model for succinoglycan biosynthesis. *J Bacteriol* **175,** 7045-7055.

Gonzalez, J. E., Reuhs, B. & Walker, G. C. (1996). Low molecular weight EPS II of *Rhizobium meliloti* allows nodule invasion in *Medicago sativa*. *Proc Natl Acad Sci U S A* **93,** 8636-8641.

Grangeasse, C., Obadia, B., Mijakovic, I., Deutscher, J., Cozzone, A. J. & Doublet, P. (2003). Autophosphorylation of the *Escherichia coli* protein kinase Wzc regulates tyrosine phosphorylation of Ugd, a UDP-glucose dehydrogenase. *J Biol Chem* **278,** 39323–39329.

Grangeasse, C., Cozzone, A., Deutscher, J. & Mijakovic, I. (2007). Tyrosine phosphorylation: an emerging regulatory device of bacterial physiology. *Trends Biochem Sci* **32,** 86-94.

Grangeasse, C., Doublet, P., Vincent, C., Vaganay, E., Riberty, M., Duclos, B. & Cozzone, A. J. (1998). Functional characterization of the low-molecular-mass phosphotyrosine-protein phosphatase of *Acinetobacter johnsonii*. *J Mol Biol* **2782,** 339-347.

Gruszczyk, J., Fleurie, A., Olivares-Illana, V., Béchet, E., Zanella-Cleon, I., Moréra, S., Meyer, P., Pompidor, G., Kahn, R., Grangeasse, C. & Nessler, S. (2011). Structure analysis of the *Staphylococcus aureus* UDP-N-acetyl-mannosamine dehydrogenase Cap5O involved in capsular polysaccharide biosynthesis. *J Biol Chem* **286,** 17112-17121.

Huang, J. & Schell, M. (1995). Molecular characterization of the *eps* gene cluster of *Pseudomonas solanacearum* and its transcriptional regulation at a single promoter. *Mol Microbiol* **16,** 977-989.

Jofré, E. & Becker, A. (2009). Production of succinoglycan polymer in *Sinorhizobium meliloti* is affected by SM21056 and requires the N-terminal domain of ExoP. *Mol Plant-Microbe Interact* **22,** 1656-1668.

Jones, K. M. (2012). Increased production of the exopolysaccharide succinoglycan enhances *Sinorhizobium meliloti* 1021 symbiosis with the host plant *Medicago truncatula*. *J Bacteriol* **194,** 4322-4331.

Keller, M., Roxlau, A., Weng, W. M., Schmidt, M., Quandt, J., Niehaus, K., Jording, D., Arnold, W. & Puhler, A. (1995). Molecular analysis of the *Rhizobium meliloti mucR* gene regulating the biosynthesis of the exopolysaccharides succinoglycan and galactoglucan. *Mol Plant-Microbe Interact* **8,** 267-277.

Kennelly, P. J. & Potts, M. (1999). Life among the primitives: Protein *O*-phosphatases in prokaryotes. *Frontiers Biosci* **4:**d372-d385.

Kennelly, P. J. (2001). Protein phosphatases -a phylogenetic perspective. *Chem Rev* **101,** 2291-2312.

Kennelly, P. J. (2002). Protein kinases and protein phosphatases in prokaryotes: a genomic perspective. *FEMS Microbiol Lett* **206,** 1-8.

Lacour, S., Bechet, E., Cozzone, A. J., Mijakovic, I. & Grangeasse, C. (2008). Tyrosine phosphorylation of the UDP-Glucose Dehydrogenase of Escherichia coli is at the crossroads of colanic acid synthesis and polymyxin resistance. *PLoS One* **3,** e3053.

Leigh, J. A. & Lee, C. C. (1988). Characterization of polysaccharides of *Rhizobium meliloti exo* mutants that form ineffective nodules. *J Bacteriol* **170,** 3327-3332.

Leigh, J. A. & Walker, G. C. (1994). Exopolysaccharides of *Rhizobium*: synthesis, regulation and symbiotic function. *Trends Genet* **10,** 63-67.

Markowitz, V. M., Korzeniewski, F., Palaniappan, K., Szeto, E., Werner, G., Padki, A., Zhao, X., Dubchak, I., Hugenholtz, P., Anderson, I., Lykidis, A., Mavromatis, K., Ivanova, N. & Kyrpides, N. C. (2006). The integrated microbial genomes (IMG) system. *Nucleic Acids Res* **34,** D344-8.

Messens, J., Hayburn, G., Desmyter, A., Laus, G. & Wyns, L. (1999). The essential catalytic redox couple in arsenate reductase from *Staphylococcus aureus*. *Biochem* **38,** 16857-16865.

Mijakovic, I., Musumeci, L., Tautz, L., Petranovic, D., Edwards, R.A., Jensen, P.R., Mustelin, T., Deutscher, J. & Bottini, N. (2005). In vitro characterization of the *Bacillus subtilis* protein tyrosine phosphatase YwqE. *J Bacteriol* **187,** 3384-3390.

Mijakovic, I., Petranovic, D., Bottini, N., Deutscher, J. & Ruhdal Jensen, P. (2005). Protein-tyrosine phosphorylation in *Bacillus subtilis*. *J Mol Microbiol Biotechnol* **9,** 189-197.

Minic, Z., Marie, C., Delorme, C., Faurie, J. M., Mercier, G., Ehrlich, D. & Renault, P. (2007). Control of EpsE, the phosphoglycosyltransferase initiating exopolysaccharide synthesis in *Streptococcus thermophilus*, by EpsD tyrosine kinase. *J Bacteriol* **189,** 1351-1357.

Moreno, E., Stackebrandt, E., Dorsch, M., Wolters, J., Busch, M. & Mayer, H. (1990). *Brucella abortus* 16S rRNA and lipid A reveal a phylogenetic relationship with members of the alpha-2 subdivision of the class Proteobacteria. *J Bacteriol* **172,** 3569-3576.

Mori, Y., Maeda, M., Takegawa, K. & Kimura, Y. (2012). PhpA, a tyrosine phosphatase of *Myxococcus xanthus*, is involved in the production of exopolysaccharide. *Microbiol* **158,** 2546-2555.

Müller, P., Hynes, M., Kapp, D., Niehaus, K. & Pühler, A. (1988). Two classes of *Rhizobium meliloti* infection mutants differ in exopolysaccharide production and in coinoculation properties with nodulation mutants. *Mol Gen Genet* **211,** 17-26.

685 **Nadler, C., Koby, S., Peleg, A., Johnson, A. C., Suddala, K. C., Sathiyamoorthy, K.,**
686 **Smith, B. E., Saper, M. A. & Rosenshine, I. (2012).** Cycling of Etk and Etp phosphorylation
687 states is involved in formation of group 4 capsule by *Escherichia coli*. *PLoS One* **7,** e37984.
688
689 **Nakar, D. & Gutnick, D. L. (2003).** Involvement of a protein tyrosine kinase in production
690 of the polymeric bioemulsifier emulsan from the oil-degrading strain *Acinetobacter iwoffii*
691 RAG-1. *J Bacteriol* **185,** 1001-1009.
692
693 **Niehaus, K. & Becker, A. (1998).** The role of microbial surface polysaccharides in the
694 *Rhizobium*-legume interaction. *Subcell Biochem* **29,** 73-116.
695
696 **Niemeyer, D. & Becker, A. (2001).** The molecular weight distribution of succinoglycan
697 produced by *Sinorhizobium meliloti* is influenced by specific tyrosine phosphorylation and
698 ATPase activity of the cytoplasmic domain of the ExoP protein. *J Bacteriol* **183,** 5163-5170.
699
700 **Paiment, A., Hocking, J. & Whitfield, C. (2002).** Impact of phosphorylation of specific
701 residues in the tyrosine autokinase, Wzc, on its activity in assembly of group 1 capsules in
702 *Escherichia coli*. *J Bacteriol* **184,** 6437-6447.
703
704 **Preneta, R., Jarraud, S., Vincent, C., Doublet, P., Duclos, B., Etienne, J. & Cozzone, A.**
705 **J. (2002).** Isolation and characterization of a protein-tyrosine kinase and a phosphotyrosine-
706 protein phosphatase from *Klebsiella pneumoniae*. *Comp Biochem Physiol B Biochem Mol*
707 *Biol* **131,** 103-112.
708
709 **Reed, J.W., Capage, M., & Walker, G.C. (1991).** *Rhizobium meliloti exoG* and *exoJ*
710 mutations affect the exoX-exoY system for modulation of exopolysaccharide production.

711 *J Bacteriol* **173,** 3776-3788.

712

713 **Reuber, T. L. & Walker, G. C. (1993).** Biosynthesis of succinoglycan, a symbiotically
714 important exopolysaccharide of *Rhizobium meliloti*. *Cell* **74,** 269-260.

715

716 **Rolfe, B. G., Gresshoff, P. M. & Shine, J. (1980).** Rapid screening for symbiotic mutants of
717 *Rhizobium* and white clover. *Plant Sci Lett* **19,** 277-284.

718

719 **Sali, A., Potterton, L., Yuan, F., van Vlijmen, H. & Karplus, M. (1995).** Evaluation of
720 comparative protein modeling by MODELLER. *Proteins* **23,** 318-326.

721

722 **Sambrook, J., Fritsch, E. F. & Maniatis, T. (1989).** Molecular Cloning: A Laboratory
723 Manual, 2nd ed. Cold Spring Harbor Laboratory Press, Cold Spring Harbor, NY, U.S.A.

724

725 **Shi, L., Potts, M. & Kennelly, P. J. (1998).** The serine, threonine, and/or tyrosine-specific
726 protein kinases and protein phosphatases of prokaryotic organisms: a family portrait. *FEMS*
727 *Microbiol Rev* **22,** 229-253.

728

729 **Skorupska, A., Janczarek, M., Marczak, M., Mazur, A. & Król, J. (2006).** Rhizobial
730 exopolysaccharides: genetic control and symbiotic functions. *Microbiol Cell Factories* **5,** 7-
731 26.

732

733 **Söding, J., Biegert, A. & Lupas, A. N. (2005).** The HHpred interactive server for protein
734 homology detection and structure prediction. *Nucleic Acids Res* **33:**W244-8.

735

Standish, A. J. & Morona, R. (2014). The role of bacterial protein tyrosine phosphatases in the regulation of the biosynthesis of secreted polysaccharides. *Antioxid Redox Signal* **20,** 2274-2289.

Standish, A. J., Salim, A. A., Zhang, H., Capon, R. J. & Morona, R. (2012). Chemical inhibition of bacterial protein tyrosine phosphatase suppresses capsule production. *PLoS One* **7,** e36312.

Tan, H., Wan, S., Liu, P. Q., Wang, L., Zhang, C. C. & Chen W. L. (2013). Alr5068, a Low-Molecular-Weight protein tyrosine phosphatase, is involved in formation of the heterocysts polysaccharide layer in the cyanobacterium *Anabaena* sp. PCC 7120. *Res Microbiol* **164,** 875-885.

Tauch, A., Zheng, Z., Pühler, A. & Kalinowski, J. (1998). *Corynebacterium striatum* chloramphenicol resistance transposon Tn5564: Genetic organization and transposition in *Corynebacterium glutamicum*. *Plasmid* **40,** 126-139.

Towbin, H., Staehelin, T. & Gordon, J. (1979). Electrophoretic transfer of proteins from polyacrylamide gels to nitrocellulose sheets: procedure and some applications. *Proc Natl Acad Sci U S A* **76,** 4350-4354.

Vincent, C., Doublet, P., Grangeasse, C., Vaganay, E., Cozzone, A. J. & Duclos, B. (1999). Cells of *Escherichia coli* contain a protein-tyrosine-kinase, Wzc, and a phosphotyrosine-protein phosphatase, Wzb. *J Bacteriol* **181,** 3472-3477.

Vincent, C., Duclos, B., Grangeasse, C., Vaganay, E., Riberty, M., Cozzone, A. J. & Doublet, P. (2000). Relationship between exopolysaccharide production and protein-tyrosine phosphorylation in gram-negative bacteria. *J Mol Biol* **304,** 311-321.

Wang, L., Wang, Y., Pellock, B. & Walker, G. C. (1999). Structural characterization of the symbiotically important low-molecular-weight succinoglycan of *Sinorhizobium meliloti*. *J Bacteriol* **181,** 6788-6796.

Whitmore, S. E. & Lamont, R. J. (2012). Tyrosine phosphorylation and bacterial virulence. *Int J Oral Sci* **4,** 1-6.

Whitfield, C. (2006). Biosynthesis and assembly of capsular polysaccharides in *Escherichia coli*. *Annu Rev Biochem* **75,** 39-68.

Yother, J. (2011). Capsules of *Streptococcus pneumoniae* and other bacteria: paradigms for polysaccharide biosynthesis and regulation. *Annu Rev Microbiol* **65,** 563-581.

Zevenhuisen, L. P. T. M. & van Neerven, A. R. W. (1983). (1,2)-β-D-Glucan and acidic oligosaccharides produced by *Rhizobium meliloti*. *Carbohydr Res* **118,** 127-134.

Zhang, Z. Y., Wang, Y., Wu, L., Fauman, E. B., Stuckey, J. A., Schubert, H. L., Saper, M. A. & Dixon, J. E. (1994). The Cys(X)5Arg catalytic motif in phosphoester hydrolysis. *Biochem* **33,** 15266-15270.

Zhang, Z-Y. (2001). Protein tyrosine phosphatases: prospects for therapeutics. *Curr Opin Chem Biol* **5,** 416-423.

787 **Table 1. Bacterial strains, plasmids and primers used in this study**

Strains	Relevant characteristics*	Reference or source
Sinorhizobium meliloti		
Rm 2011	Wild type; Nod+, Fix+, Inf+, EPS+, Nx^r, Sm^r	(J. Dénarié, France)
Rm42	Nonpolar SMc02309 mutant in Rm2011, Nm^r, Nx^r	This work
Rm43	Rm42 carrying pFAJ-02309, Nm^r, Tc^r, Nx^r	This work
Rm148	Rm2011 carrying pFAJ1708, Tc^r, Nx^r	This work
RmAR9007	Rm2011, *exoY-lacZ*/*aacC*1, Gm^r, Nx^r	(Keller *et al.,* 1995)
Plasmids		
pTYB1	Expression vector generating intein fusion proteins, Ap^r	New England BioLabs
pET28 a(+)	Expression vector generating 6x His fusion proteins, Km^r	Novagen
pGEX 5x-1	Expression vector generating glutathione*S*-transferase (GST) fusion proteins; Ap^r	Amersham Biosciences
pK18mob2	pK18mob derivative with unique *Kpn*I and *Sac*I sites in the multiple cloning site; Km^r	(Tauch *et al.,* 1998)
pK18-02309	pK18mob2 derivative carrying a 187-bp internal fragment of SMc02309 gene from Rm 2011 cloned into the *EcoR*I and *Hind*III sites, Km^r	This work
pFAJ1708	Broad-host-range plasmid with *nptII* promoter used for overexpression; Tc^r	(Daniels *et al.*, 2006)
pFAJ-02309	pFAJ1708 derivative carrying the ORF SMc02309of Rm2011, cloned in *Xba*I/*Kpn*I sites; Tc^r	This work
pGEX-exoPc	pGEX-5x-1 carrying the 925-bp *exoP*3´ portion and 70 bp of the intergeneic region; Ap^r	(Niemeyer & Becker, 2001)
pTYB-02309	pTYB1 derivative carrying the ORF SMc02309 of Rm2011, cloned in *Nde*I/*Sap*I sites; Ap^r	This work
pET28-exoN	pET28 a(+) derivative carrying *exoN* of Rm2011, cloned in *Nde*I/*BamH*I sites; Km^r.	This work
Primers	**Sequence (5´-3´)§**	
2309f	GGTGGTCATATGATCGCGACCGCGATGCC	This work

2309r	GGTGGTTGCTCTTCCGCATGCCGCCGGAG GACTGCCT	This work
pK2309f	CGGAATTCATCCCTTCGTGGACGTGGTT	This work
pK2309r	GGTAAGCTTTCGGGTGTCGGCCAATATA	This work
pFAJ2309f	GCTCTAGAATGATCGCGACCGCGATGCC	This work
pFAJ2309r	GGGGTACCTCATGCCGCCGGAGGACTGC	This work
exoNf	GGTGGTCATATGGACCGTGTCAGGACCGT	This work
exoNr	CGGGATCCTTATGCCGCCCGGATGCGGC	This work

788 *Nx^r, Sm^r, Nm^r, Gm^r, Ap^r, Tc^r and Km^r = resistant to nalidixic acid, streptomycin, neomycin,

789 gentamicin, ampicillin, tetracycline and kanamycin, respectively.

790 §Restriction sites are underlined.

791

792 **Table 2. Effects of phosphatase inhibitors on SMc02309 activity**

Phosphatase inhibitor	**% Relative activity ± SD**
No inhibitor	100.00 ± 5.66
Na_3VO_4 (1 mM)	44.53 ± 1.69
Na_3VO_4 (2.5 mM)	32.74 ± 9.12
$NaPP_i$ (1 mM)	79.75 ± 1.77
$NaPP_i$ (2.5 mM)	65.95 ± 4.53

793

Table 3. UDP-glucose pyrophosphorylase activity of ExoN after tyrosine dephosphorylation.

Reaction	**Specific activity (μmol min^{-1} mg^{-1}) ± SD**
ExoN	0.38 ± 0.0108
ExoN + SMc02309	0.23 ± 0.0043
ExoN + ALP	0.14 ± 0.0103

UDP-glucose pyrophosphorylase activity was monitored at 340 nm for 15 min by measuring NADPH formation by ExoN and ExoN previously treated with SMc02309 phosphatase or by commercial alkaline phosphatase (ALP).

802 **Figures Legends**

803 **Fig. S1. a,** Synteny analysis of the *exoP* gene (grey) from *S. meliloti* and others BY-K genes
804 of *Escherichia coli* K-12, *Acinetobacter johnsonii*, *Erwinia amylovora, Klebsiella pneumonia,*
805 *Ralstonia solanacearum* and *Burkholderia* sp. Genes encoding LMW-PTP proteins (black)
806 are mainly located upstream from BY-K genes except in *S. meliloti*. **b,** Synteny analysis of the
807 SMc2309 gene (black) in *S. meliloti* and others LMW-PTP genes of related bacteria like
808 *Rhizobium leguminosarum* bv. *trifolii* WSM1325, *Mesorhizobium loti* MAFF303099,
809 *Ochrobactrum anthropi* ATCC 49188, *Brucella abortus* A13334, *Brucella melitensis* bv.
810 *abortus* 2308 and *Bradyrhizobium japonicum* USDA110. Arrows at lower levels indicate that
811 the coding sequences are located in the minus strand. **c,** The regions containing the conserved
812 residues in the active site of SMc02309 and the DPY motif are compared with the
813 corresponding region of several members of the LMW-PTP family. They include BceF of
814 *Burkholderia cepacia*, AmsI of *E. amylovora*, Wzb of *E. coli*, EspP of *R. solanacearum*, and
815 Ptp of *A. johnsonii*. The LMW protein phosphatase encoded by locus tag
816 Q57FA1/BruAb1_0278 of *B. abortus* is also included.

817

818 **Fig. S2**. Rooted phylogenetic tree of SMc02309 protein. The tree was constructed using
819 CLUSTAL W (available at http://www.expasy.ch/) and visualized with FigTree version 1.4
820 (http://tree.bio.ed.ac.uk/software/figtree). SMc02309 comparison includes the follow LMW-
821 PTPs: YFKJ and YWLE of *Bacillus subtilis*, Q8YM72 of *Anabaena* sp., PtpA of
822 *Mycobacterium tuberculosis*, PtpA of *Streptomyces coelicolor*, Wzb and Etp of *E. coli*, AmsI
823 of *Erwinia amylovora*, EspP of *Ralstonia solanacearum*, BceD of *Burkholderia cepacia*, Ptp
824 of *Acinetobacter johnsonii* and Q57FA1 of *Brucella abortus.* Also the follow arsenate
825 reductases: ArsC of *Bacillus subtilis*, ArsC of *Staphylococcus aureus*, P74313 of
826 *Synechocystis* sp., Q9A861 of *Caulobacter crescentus*, MGSR of *Bacillus subtilis*, Q9HXX5
827 of *Pseudomonas aeruginosa*, Q2YMA4 *of Brucella abortus*, YFFB of *E. coli*, Q8Z0A3 of

828 *Anabaena* sp., Q9K785 of *Bacillus halodurans*, Q9KQ39 of *Vibrio cholerae*, ArsC of
829 *Shigella flexneri*, D0S8B1 of *Acinetobacter johnsonii*, Q98J03 of *Rhizobium loti* and ArsC of
830 *S. meliloti* are included. HPRK of *Bacillus subtilis* was used as outgroup since it was a
831 phylogenetically distant protein.
832
833 **Fig. 1. a,** Overexpression of SMc02309 gene. The SMc02309 intein-tagged protein was
834 produced in *E. coli* BL21(DE3) and separated by SDS-PAGE. Lanes1: molecular weight
835 marker; 2: proteins from uninduced *E. coli* BL21(DE3) cells harbouring pTYB1- SMc02309
836 gene; 3: proteins after induction with 0.5 mM IPTG; 4: after purification with chitin beads and
837 cleavage with DTT, a 17 kDa protein was visualized. **b,** Mass spectra of peptides resulting
838 from trypsin digestion of the protein SMc02309 as a function of mass/charge ratio.
839
840 **Fig. 2. a,** Saturation curves of LMW-PTP SMc02309 of *S. meliloti* by *p*-NPP in the presence
841 of 0.1 mM Zn^{2+}. After 60 min at 37°C, the reactions were stopped with 1M NaOH. Bars show
842 SD. **b,** Effect of pH. The reactions were carried out at 37 °C using 7 mM *p*-NPP dissolved in
843 20 mMAcH/AcNa pH 4.2 or in 20 mM sodium citrate buffer pH 5.5, 6, 6.5, 7 and 7,5 with 40
844 µg enzyme in presence of Zn^{2+}. **c,** Effect of temperature. The reactions were carried out at 30,
845 37, 45, 55, 65 and 75 °C using 7 mM *p*-NPP as substrate in 20 mM sodium citrate pH 6 with
846 40 µg enzyme in presence of Zn^{2+}.
847
848 **Fig. 3.** Dephosphorylation assays of **a,** ExoPc and **b,** ExoN by SMc02309 phosphatase.
849 Purified ExoPc and ExoN proteins were incubated with SMc02309 protein and tested for
850 tyrosine dephosphorylation by immunoblotting using anti-ExoPc (anti-ExoP), Anti-His, and
851 anti-phosphotyrosine (Anti-P-Tyr) antibodies, respectively. A decreased pattern of
852 phosphorylation was observed when ExoN was incubated with SMc02309. When both ExoPc

and ExoN proteins were incubated with commercial phosphatase (ALP), complete tyrosine dephosphorylation was observed.

Fig. 4. Production of EPS I by *S. meliloti* strains Rm2011 (wild type), Rm42 (SMc02309 mutant), Rm43 (SMc02309 mutant complemented with pFAJ-02309), Rm148 (wild type carrying empty vector pFAJ1708) and RmAR9007 (*exoY* mutant deficient in EPS I production). EPS I was obtained from supernatants of 6 days-old cultures grown in glutamate-D-mannitol-salts (GMS) medium supplemented with 240 mM NaCl. Bars represent the means of three biological replicates with two technical replicates each ± SD. ** $p<0.05$ relative to Rm2011 (WT).

Fig. 5. Nodulation pattern of *S. meliloti* strains Rm2011 and Rm42. Seed were surface sterilized, germinated and inoculated as described in materials and methods. Nodules formation was monitored during four weeks. All nodules were pink. Bars indicate SD. ** $p<0.05$. n=13.

Figure 1

Click here to download Figure Fig 1.tif

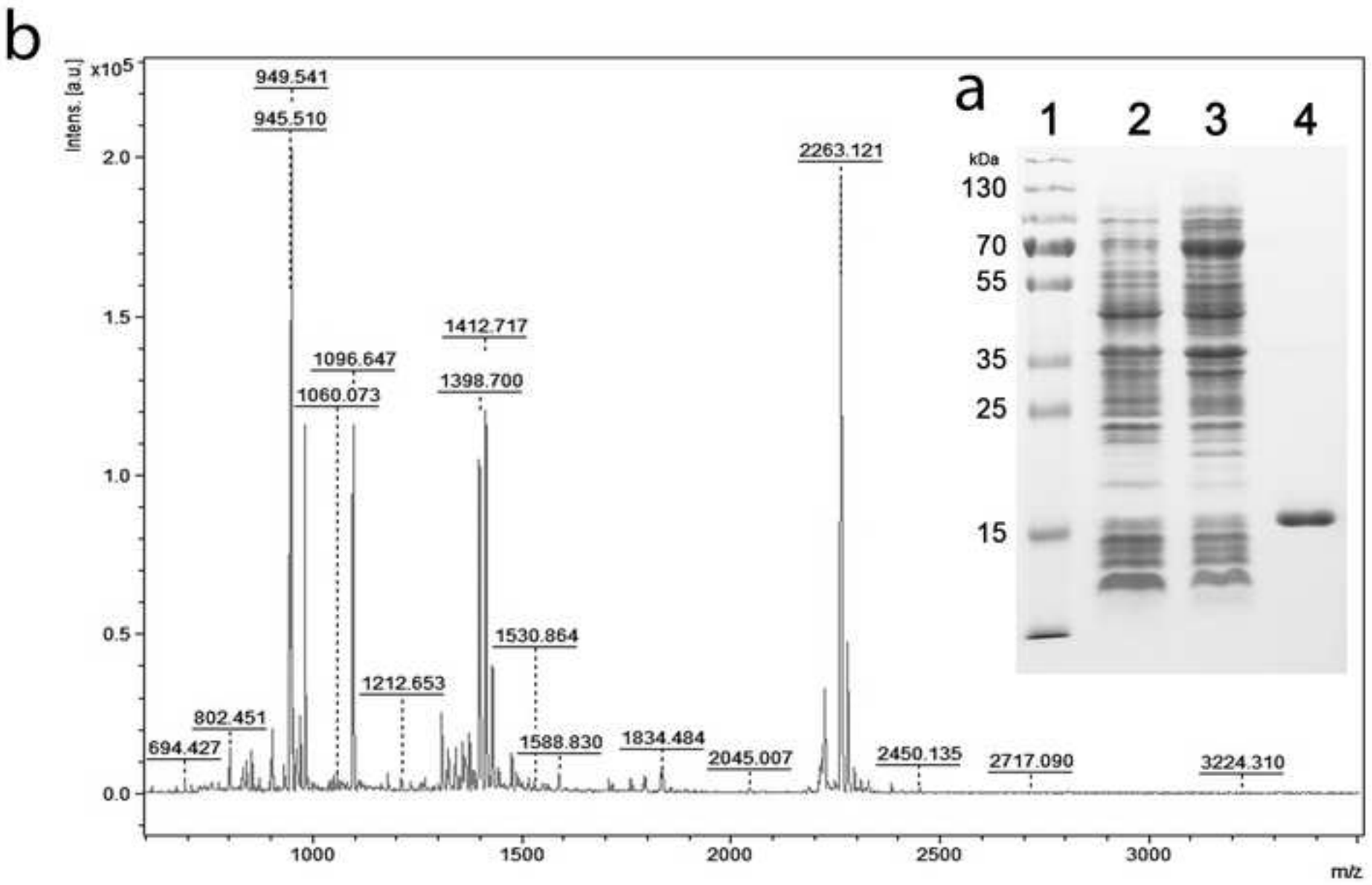

Figure 2

Click here to download Figure Fig 2.tif

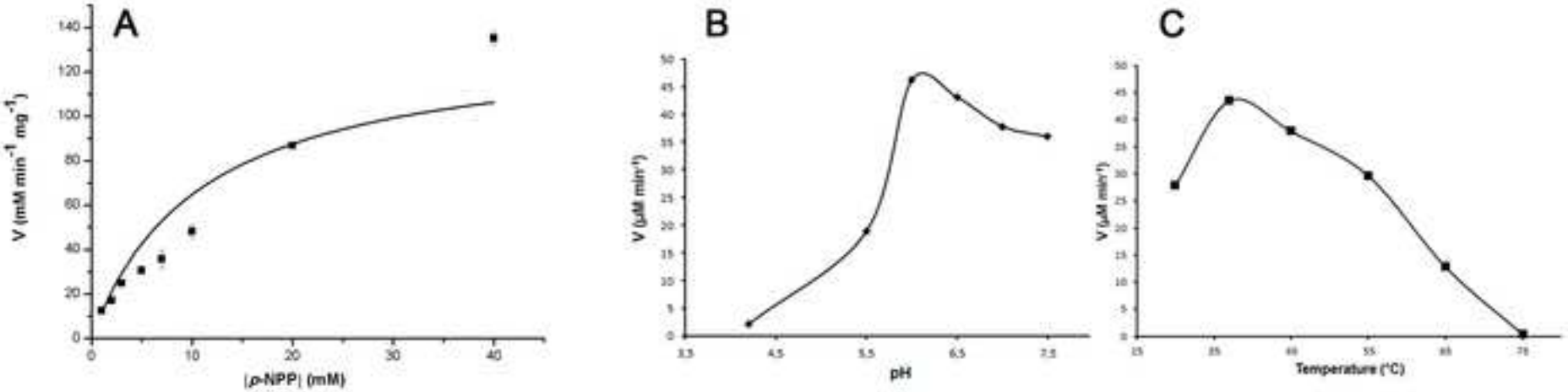

Figure 3

Click here to download Figure Fig 3.tif

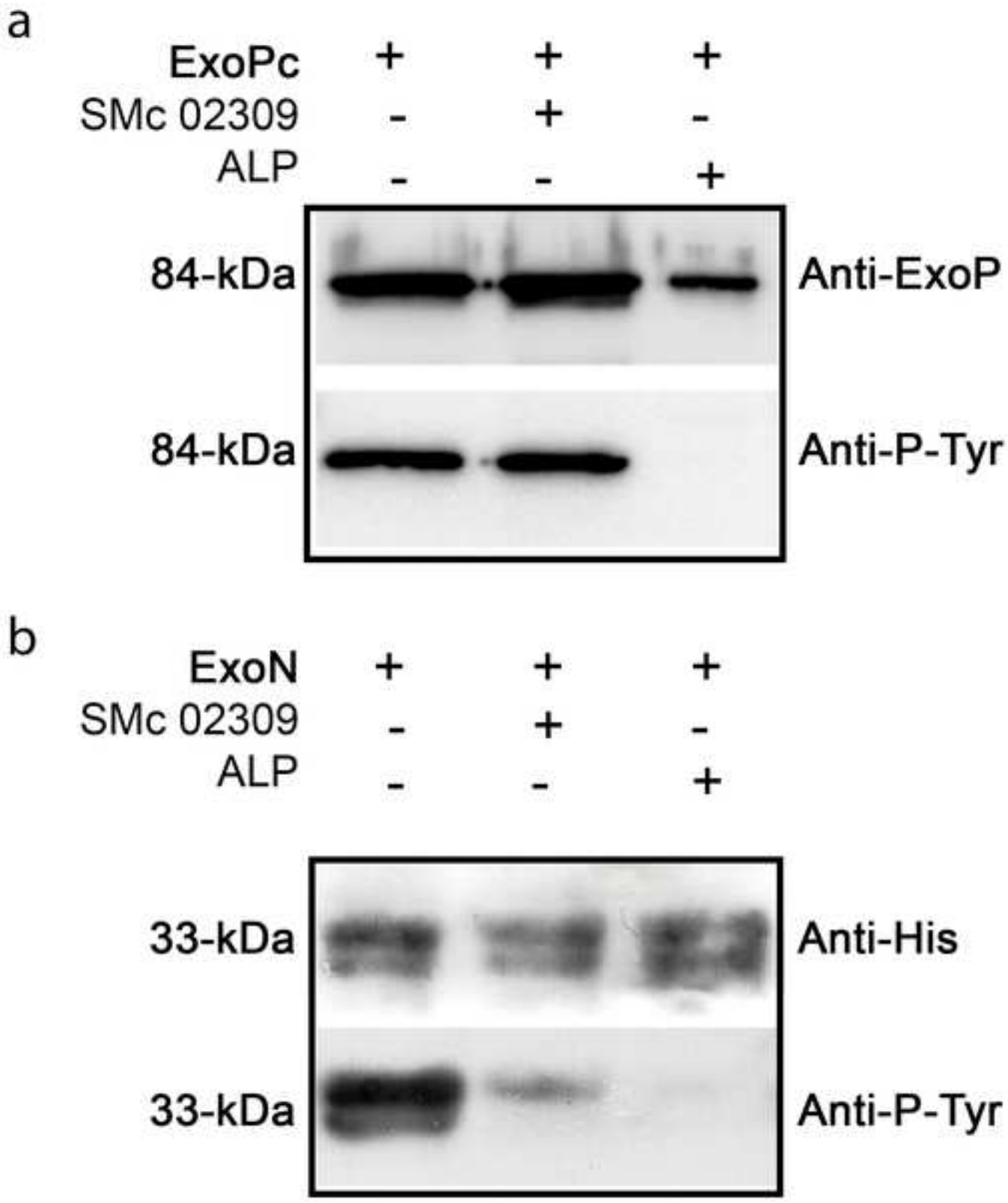

Figure 4

Click here to download Figure Fig 4.tif

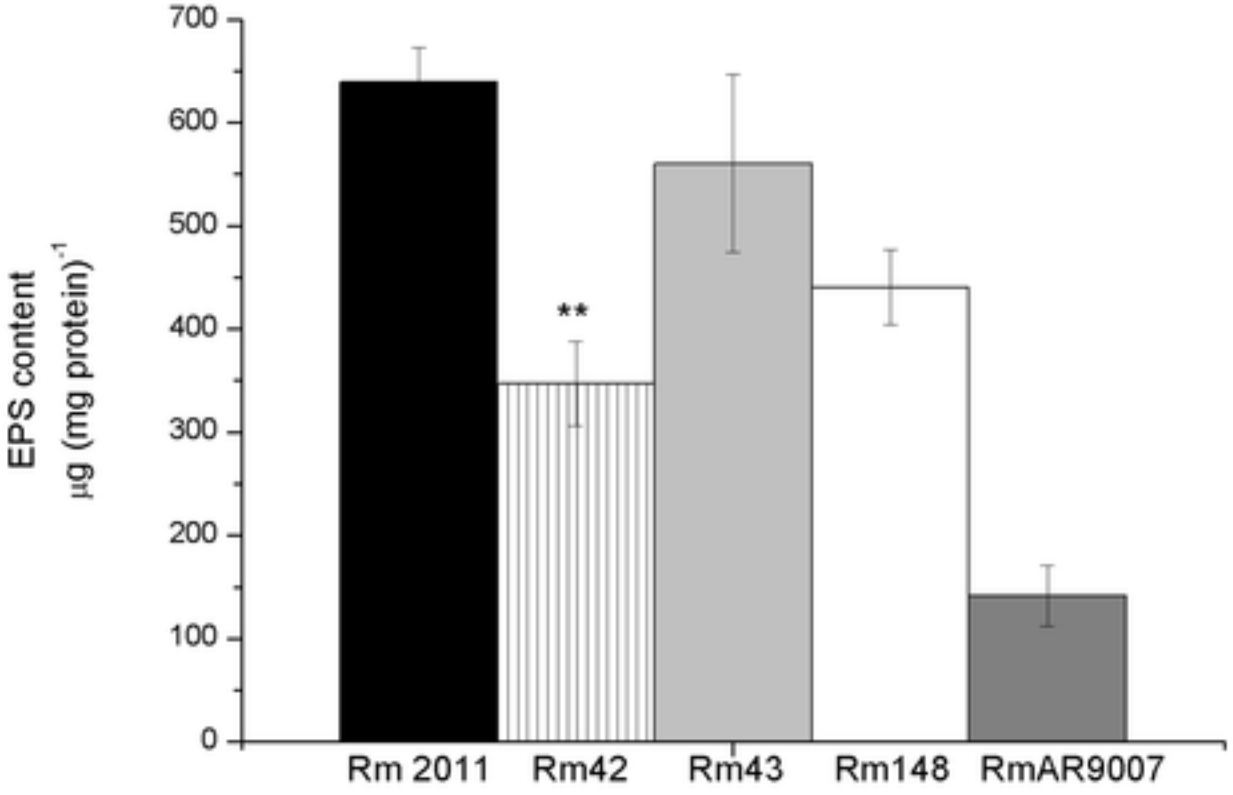

Figure 5

Click here to download Figure Fig 5.tif

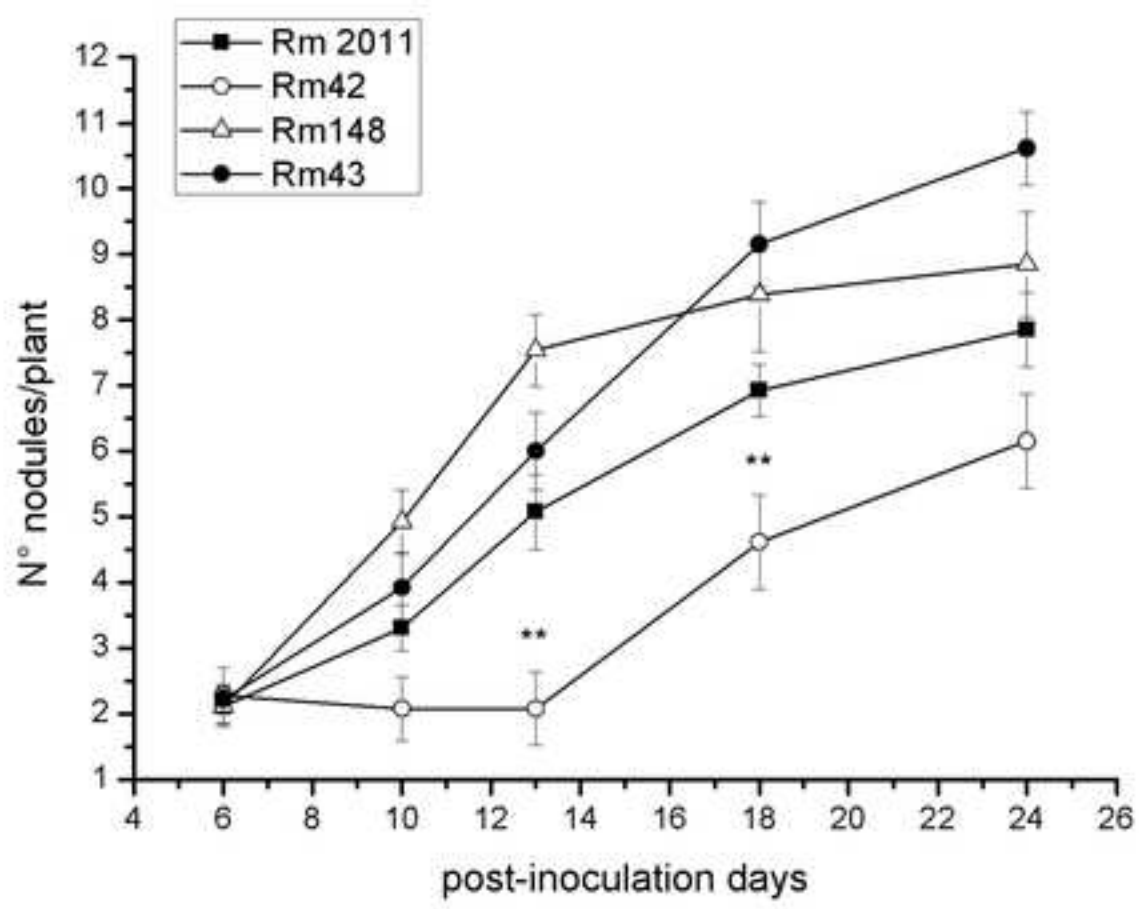

Supplementary Figures

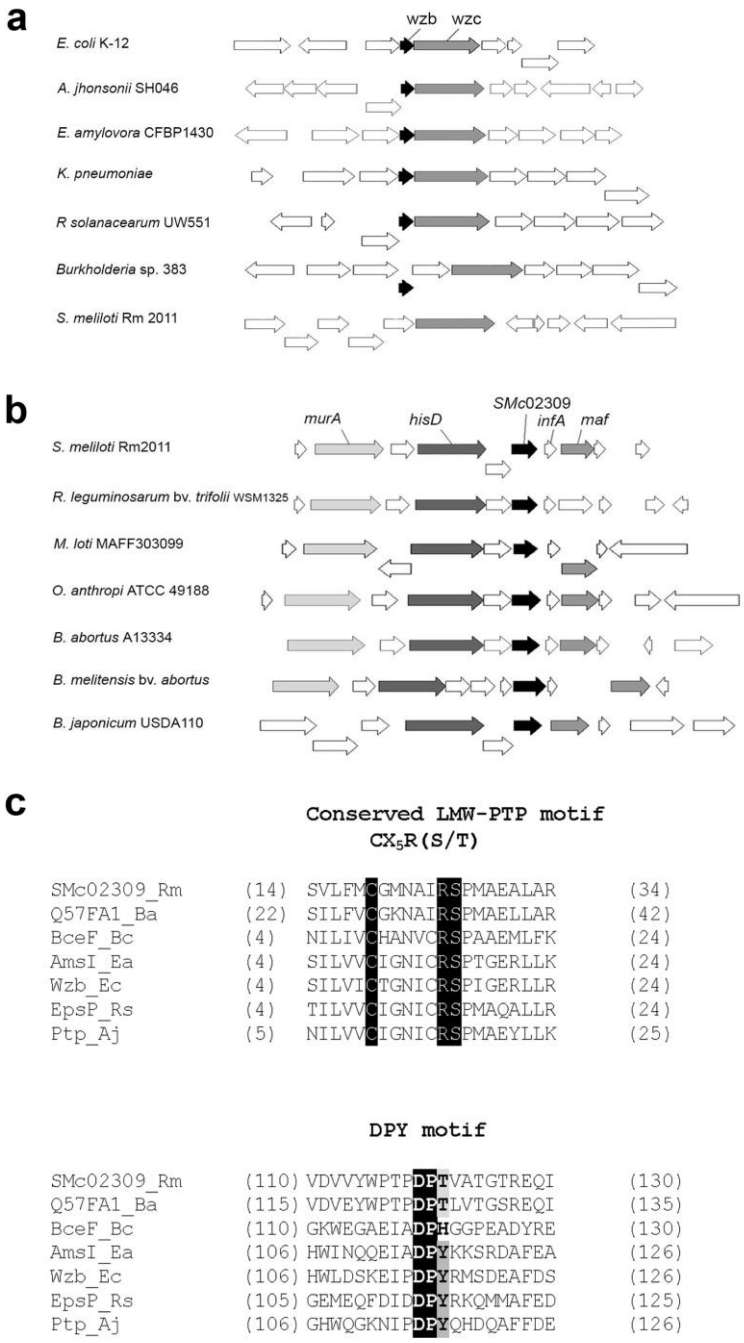

Fig. S1. a, Synteny analysis of the *exoP* gene (grey) from *S. meliloti* and others BY-K genes of *Escherichia coli* K-12, *Acinetobacter johnsonii*, *Erwinia amylovora*, *Klebsiella pneumonia*, *Ralstonia solanacearum* and *Burkholderia* sp. Genes encoding LMW-PTP proteins (black) are mainly located upstream from BY-K genes except in *S. meliloti*. **b,**

Synteny analysis of the SMc2309 gene (black) in *S. meliloti* and others LMW-PTP genes of related bacteria like *Rhizobium leguminosarum* bv. *trifolii* WSM1325, *Mesorhizobium loti* MAFF303099, *Ochrobactrum anthropi* ATCC 49188, *Brucella abortus* A13334, *Brucella melitensis* bv. *abortus* 2308 and *Bradyrhizobium japonicum* USDA110. Arrows at lower levels indicate that the coding sequences are located in the minus strand. **c,** The regions containing the conserved residues in the active site of SMc02309 and the DPY motif are compared with the corresponding region of several members of the LMW-PTP family. They include BceF of *Burkholderia cepacia*, AmsI of *E. amylovora*, Wzb of *E. coli*, EspP of *R. solanacearum*, and Ptp of *A. johnsonii*. The LMW protein phosphatase encoded by locus tag Q57FA1/BruAb1_0278 of *B. abortus* is also included.

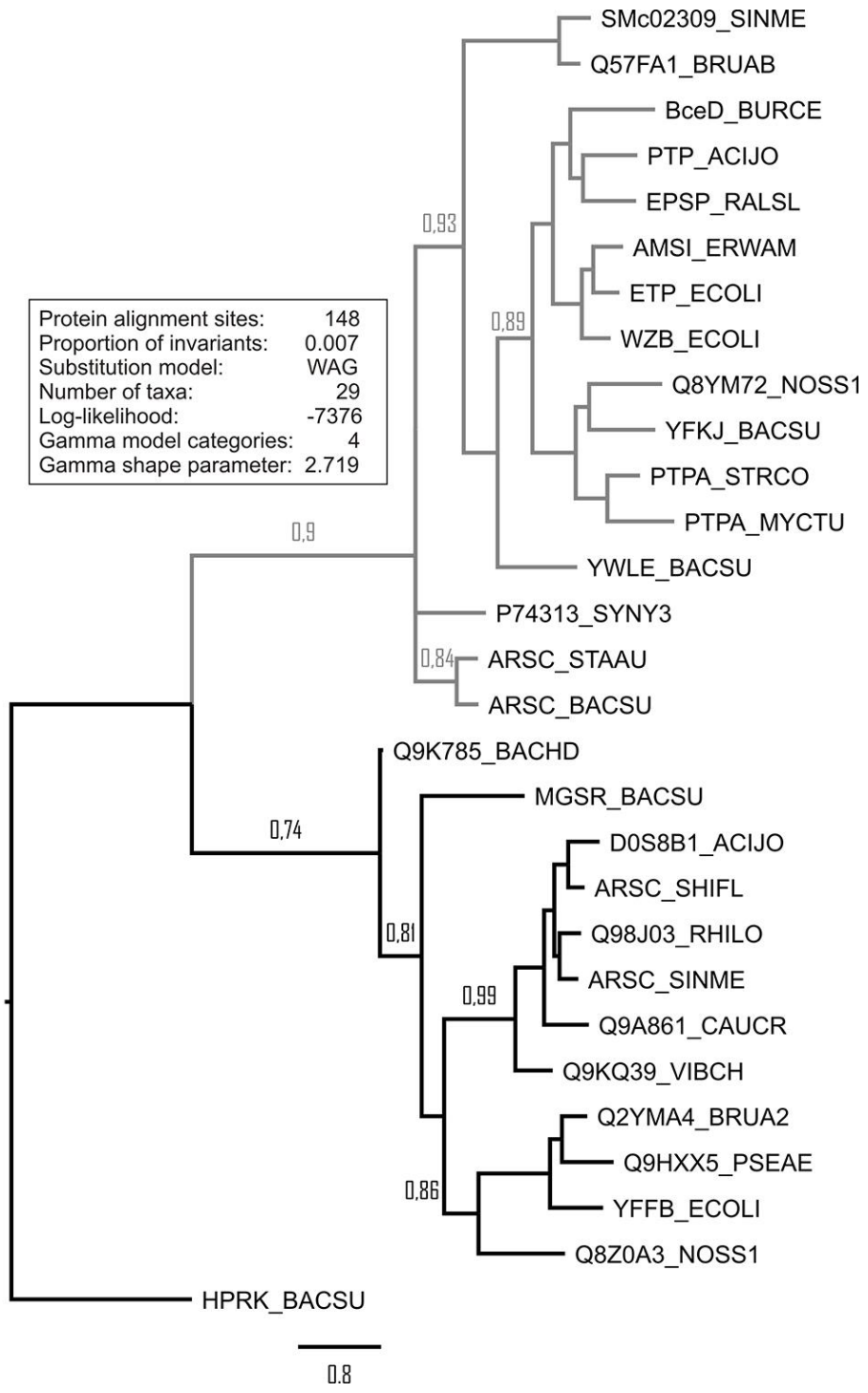

Fig. S2. Rooted phylogenetic tree of SMc02309 protein. The tree was constructed using CLUSTAL W (available at http://www.expasy.ch/) and visualized with FigTree version 1.4 (http://tree.bio.ed.ac.uk/software/figtree). SMc02309 comparison includes the follow LMW-PTPs: YFKJ and YWLE of *Bacillus subtilis*, Q8YM72 of *Anabaena* sp., PtpA of *Mycobacterium tuberculosis*, PtpA of *Streptomyces coelicolor*, Wzb and Etp of

E. coli, AmsI of *Erwinia amylovora*, EspP of *Ralstonia solanacearum*, BceD of *Burkholderia cepacia*, Ptp of *Acinetobacter johnsonii* and Q57FA1 of *Brucella abortus.* Also the follow arsenate reductases: ArsC of *Bacillus subtilis*, ArsC of *Staphylococcus aureus*, P74313 of *Synechocystis* sp., Q9A861 of *Caulobacter crescentus*, MGSR of *Bacillus subtilis*, Q9HXX5 of *Pseudomonas aeruginosa*, Q2YMA4 *of Brucella abortus*, YFFB of *E. coli*, Q8Z0A3 of *Anabaena* sp., Q9K785 of *Bacillus halodurans*, Q9KQ39 of *Vibrio cholerae*, ArsC of *Shigella flexneri*, D0S8B1 of *Acinetobacter johnsonii*, Q98J03 of *Rhizobium loti* and ArsC of *S. meliloti* are included. HPRK of *Bacillus subtilis* was used as outgroup since it was a phylogenetically distant protein.